Work Fluctuations for a Harmonically Confined Active Ornstein-Uhlenbeck Particle

Massimiliano Semeraro, Giuseppe Gonnella, Antonio Suma, and Marco Zamparo

Dipartimento Interateneo di Fisica, Università degli Studi di Bari and INFN, Sezione di Bari, via Amendola 173, Bari I-70126, Italy

(Received 21 February 2023; accepted 13 September 2023; published 12 October 2023)

We study the active work fluctuations of an active Ornstein-Uhlenbeck particle in the presence of a confining harmonic potential. We tackle the problem analytically both for stationary and generic uncorrelated initial states. Our results show that harmonic confinement can induce singularities in the active work rate function, with linear stretches at large positive and negative active work, at sufficiently large active and harmonic force constants. These singularities originate from big jumps in the displacement and in the active force, occurring at the initial or ending points of trajectories and marking the relevance of boundary terms in this problem.

DOI: 10.1103/PhysRevLett.131.158302

Large deviation theory has a profound impact in statistical physics [1,2]. In nonequilibrium systems, where probability measures on configuration spaces are not naturally available, it provides an analog of the usual equilibrium free-energy description. Given an extensive physical observable W_τ computed by cumulating a large number τ of microscopic events, if a large deviation principle holds, then the asymptotics of the probability distribution $P(W_\tau/\tau = w)$ can be characterized by the rate function $I(w) = -\lim_{\tau\uparrow\infty}(1/\tau)\ln P(W_\tau/\tau = w)$ [3,4]. The probability distribution is dominated by small fluctuations around the minimum of I, which in this sense plays a role similar to a free-energy.

A modern important topic is the occurrence of singularities in rate functions, which can be seen as the hallmarks of phase transitions [2,5]. They appear in different contexts, such as in studies of heat exchanges, diffusive transport, and entropy production [6–20], and in some cases have been interpreted as due to a condensation mechanism [21–28]. If τ is a time interval, the rate function can provide a generalized thermodynamic description based on the counting of trajectories, and the singularity would correspond to a phase separation in trajectory space [29–31].

Active matter systems [32], with their inherent nonequilibrium character, offer a new field for applications of large deviation theory and investigations on dynamical phase transitions. In these systems, available energy sources are employed to produce spontaneous motion or work on the environment. They are characterized by a surprisingly rich phenomenology, including new phenomena like motility induced phase separation (MIPS) [33] or spontaneous flow [32], and also concerning fluctuation properties [34–43].

A central quantity for the description of dynamical transitions in active matter models is the active work. This quantity is defined as the time-average of the power of a particle's propulsion force and measures the conversion of self-propulsion into directed motion [44]. Active work enters the definition of efficiency in active engines [44], i.e., devices which exploit active nonequilibrium dynamics to produce useful work [45], as the effective power input. These devices either cyclically operate between different thermal baths [46–48] or exploit ratchet potentials [49], and already have several experimental realizations [46,47]. In this respect, active work deserves deeper investigation, not only in terms of mean values but also at the level of fluctuations, even in simple but significant setups. Numerically, in dilute systems of active Brownian particles, the active work rate function was shown to be singular [35], with a linear tail associated to trajectories of a particle being dragged by a cluster moving oppositely to its propulsion force. Successive studies have revealed a very rich structure for the phase diagram in trajectory space [50–52]. In experiments, rate functions for quantities analogous to the active work were investigated for polar beads embedded in two-dimensional granular layers [53,54].

Rigorous analysis of simple models can help to understand the emergence of dynamical transitions, and in particular to elucidate the role of self-propulsion. In this Letter we consider a single active Ornstein-Uhlenbeck particle (AOUP) [55–64] and investigate analytically the active work fluctuations in the presence of a confining harmonic potential. AOUP systems share many of the relevant properties of interacting active particle models, including MIPS. Restricting to one particle description, a confining potential can mimic the trapping created by other particles at finite densities [55,65,66]. We will show that, differently from the case of a free AOUP [67], harmonic confinement can induce singularities in the active work rate function, with linear stretches at large active work. These singularities are found both for stationary and generic uncorrelated initial states at sufficiently large active and harmonic force constants. They originate from big jumps in the displacement and in the active force, occurring at the initial or ending points of trajectories and marking the relevance of boundary terms in this problem.

The unidimensional active particle model that we study is defined via the Ornstein-Uhlenbeck process

$$\begin{cases} \gamma\dot{r}(t) = a(t) - kr(t) + \sqrt{2\gamma k_B T}\xi(t), \\ \dot{a}(t) = -\nu a(t) + F\sqrt{2\nu}\eta(t), \end{cases} \tag{1}$$

where $r(t)$ is the position of a unit-mass particle in a harmonic potential of elastic constant k, $a(t)$ represents a self-propulsion force with amplitude F and decay rate ν, γ and T are the friction coefficient and the bath temperature, and $\xi(t)$ and $\eta(t)$ are two independent standard white noises. One has $\nu \equiv k_B T/\gamma d^2$ with d a length proportional to the particle's diameter [68]. We will vary the adimensional elastic constant $\kappa \equiv (kd^2)/(k_B T)$ and the Péclet number $\mathrm{Pe} \equiv (Fd)/(k_B T)$, which quantify the strength of the potential and of the active force with respect to thermal fluctuations [68,69]. Without loss of generality, we set $\gamma = 1$, $k_B T = 1$, and $d = 1$.

We examine the probability distribution of the *active work* W_τ defined by the formula [70]

$$W_\tau \equiv \int_0^\tau a(t)\dot{r}(t)dt.$$

Our goal is to evaluate the rate function $I(w) = -\lim_{\tau\uparrow\infty}(1/\tau)\ln P(W_\tau/\tau = w)$. The probability distribution $P(W_\tau/\tau = w)$ can be expressed by the path integral

$$P(W_\tau/\tau = w) = \int \delta(W_\tau - w\tau)\mathcal{P}_\tau \mathcal{D}r\mathcal{D}a$$

with path probability

$$\mathcal{P}_\tau \propto \exp\left\{-\frac{1}{2}\begin{pmatrix} r(0) & a(0) \end{pmatrix}\Sigma_0^{-1}\begin{pmatrix} r(0) \\ a(0) \end{pmatrix}\right\}\exp\left\{-\int_0^\tau \left(\frac{[\dot{r}(t) - a(t) + \kappa r(t)]^2}{4} + \frac{[\dot{a}(t) + a(t)]^2}{4\mathrm{Pe}^2}\right)dt\right\}.$$

$\mathcal{P}_\tau$ combines the distribution of the initial values $r(0)$ and $a(0)$ with the Onsager-Machlup weight [71]. We consider Gaussian initial data with mean zero and joint covariance matrix Σ_0. In particular, we focus on a nonstationary uncorrelated initial condition with standard deviations σ_r for $r(0)$ and σ_a for $a(0)$, and on the stationary case given by [72]

$$\Sigma_0 = \begin{pmatrix} \frac{1+\kappa+\mathrm{Pe}^2}{\kappa(1+\kappa)} & \frac{\mathrm{Pe}^2}{1+\kappa} \\ \frac{\mathrm{Pe}^2}{1+\kappa} & \mathrm{Pe}^2 \end{pmatrix}. \tag{2}$$

An operative definition of the rate function I requires us to look first at a discrete-time problem with time step ϵ, and then to take the continuum limit $\epsilon\downarrow 0$. In fact, we determine I via the double limit $I(w) = -\lim_{\epsilon\downarrow 0}\lim_{N\uparrow\infty}(1/N\epsilon)\ln P(W_N/N\epsilon = w)$, where $W_N \equiv \frac{1}{2}\sum_{n=1}^N (a_n + a_{n-1})(r_n - r_{n-1})$ with $r_n \equiv r(n\epsilon)$ and $a_n \equiv a(n\epsilon)$ is the discretized active work up to time $N\epsilon$. The discrete-time problem is tackled by computing the cumulant generating function (CGF) $(1/N)\ln\langle e^{\lambda W_N}\rangle$ of W_N at large N. The Legendre transform of $\lim_{N\uparrow\infty}(1/N)\ln\langle e^{\lambda W_N}\rangle$ with respect to the additional variable λ is expected to be the discrete-time rate function $J(w) = -\lim_{N\uparrow\infty}(1/N)\ln P(W_N/N = w)$. We have $I(w) = \lim_{\epsilon\downarrow 0} J(\epsilon w)/\epsilon$.

At small ϵ, the trajectory $\{(r_0, a_0), \dots, (r_N, a_N)\}$ follows a multivariate Gaussian law with mean zero and covariance matrix Σ_N [73]. Regarding W_N as a quadratic functional of $\{(r_0, a_0), \dots, (r_N, a_N)\}$ with coefficient matrix $\frac{1}{2}\mathsf{M}_N$, a standard Gaussian integral gives

$$\ln\langle e^{\lambda W_N}\rangle = -\frac{1}{2}\ln\det(\Sigma_N^{-1} - \lambda\mathsf{M}_N) - N\ln(2\epsilon\mathrm{Pe}) - \frac{1}{2}\ln\det\Sigma_0$$

if $\Sigma_N^{-1} - \lambda\mathsf{M}_N$ is positive definite and $\ln\langle e^{\lambda W_N}\rangle = +\infty$ otherwise. $\Sigma_N^{-1} - \lambda\mathsf{M}_N$ is the block tridiagonal matrix

$$\Sigma_N^{-1} - \lambda\mathsf{M}_N = \begin{pmatrix} L & V^\top & & & \\ V & U & \ddots & & \\ & \ddots & \ddots & \ddots & \\ & & \ddots & U & V^\top \\ & & & V & R \end{pmatrix} \tag{3}$$

with 2×2 blocks $L \equiv \Sigma_0^{-1} + S^\top D^{-2}S + \lambda E_+$, $U \equiv D^{-2} + S^\top D^{-2}S$, $R \equiv D^{-2} - \lambda E_+$, $V \equiv -D^{-2}S - \lambda E_-$, $S \equiv \begin{pmatrix} 1-\kappa\epsilon & \epsilon \\ 0 & 1-\epsilon \end{pmatrix}$, $D \equiv \begin{pmatrix} \sqrt{2\epsilon} & 0 \\ 0 & \mathrm{Pe}\sqrt{2\epsilon} \end{pmatrix}$, and $E_\pm \equiv \frac{1}{2}\begin{pmatrix} 0 & 1 \\ \pm 1 & 0 \end{pmatrix}$. The matrix (3) differs from a Toeplitz matrix by the extreme diagonal blocks L containing Σ_0 and R, which play an important role in determining positive definiteness. We denote by T_N the bulk Toeplitz matrix obtained from $\Sigma_N^{-1} - \lambda\mathsf{M}_N$ by deleting all contour blocks.

For those values of λ that make $\Sigma_N^{-1} - \lambda\mathsf{M}_N$ positive definite at large N, the asymptotic CGF depends only on the bulk matrix T_N. In fact, the results of [74] for generic quadratic functionals based on Szegö theorem for block

Toeplitz matrices [77] show that $\lim_{N\uparrow\infty}(1/N)\ln\langle e^{\lambda W_N}\rangle = \varphi(\lambda)$ with

$$\varphi(\lambda) \equiv -\frac{1}{4\pi}\int_0^{2\pi} \ln\det F_\lambda(\theta)d\theta - \ln(2\epsilon\mathrm{Pe})$$

and Hermitian matrix $F_\lambda(\theta) \equiv V e^{-\mathrm{i}\theta} + U + V^\top e^{\mathrm{i}\theta}$. For $\Sigma_N^{-1} - \lambda \mathsf{M}_N$ being positive definite it is necessary and sufficient that both T_N and its Schur complement

$$\mathsf{S}_N \equiv \begin{pmatrix} L - V^\top(\mathsf{T}_N^{-1})_{11}V & -V^\top(\mathsf{T}_N^{-1})_{1N}V^\top \\ -V(\mathsf{T}_N^{-1})_{N1}V & R - V(\mathsf{T}_N^{-1})_{NN}V^\top \end{pmatrix}$$

are positive definite, $(\mathsf{T}_N^{-1})_{ij}$ being the 2×2 block of T_N^{-1} in the row i and column j. The matrix T_N is positive definite if $F_\lambda(\theta)$ has the same property for all θ [74]. This introduces a first constraint on λ, which defines the *primary domain* $(\tilde{l}_-, \tilde{l}_+)$ of φ. It can be shown [74] that $\lim_{N\uparrow\infty}\mathsf{S}_N = \left(\begin{smallmatrix}\mathcal{L}_\lambda & 0\\ 0 & \mathcal{R}_\lambda\end{smallmatrix}\right)$, $\mathcal{L}_\lambda$ and $\mathcal{R}_\lambda$ being 2×2 symmetric matrices determined by the extreme diagonal blocks L and R and by $F_\lambda(\theta)$, whose explicit expressions in the limit $\epsilon\downarrow 0$ is reported in [73]. Then, a second constraint on λ comes from the requirement that $\mathcal{L}_\lambda$ and $\mathcal{R}_\lambda$ are positive definite. Denoting by (l_-, l_+) the interval of λ for which both constraints are fulfilled, i.e., the *effective domain* of φ, we get $\lim_{N\uparrow\infty}(1/N)\ln\langle e^{\lambda W_N}\rangle = \varphi(\lambda)$ for $\lambda \in (l_-, l_+)$ and $\lim_{N\uparrow\infty}(1/N)\ln\langle e^{\lambda W_N}\rangle = +\infty$ for $\lambda \notin [l_-, l_+]$. We have $\tilde{l}_- \le l_- < 0 < l_+ \le \tilde{l}_+$.

We now compute the discrete-time rate function as the Legendre transform $J(w) = \sup_{\lambda\in(l_-,l_+)}\{w\lambda - \varphi(\lambda)\}$. Although natural, this formula cannot be justified by the Gärtner-Ellis theorem [3,4] since, in general, φ is not steep at the boundary of the effective domain. In fact, the Gärtner-Ellis theorem requires that $\lim_{\lambda\downarrow l_-}\varphi'(\lambda) = -\infty$ and $\lim_{\lambda\uparrow l_+}\varphi'(\lambda) = +\infty$, but this fails when $l_- > \tilde{l}_-$ or $l_+ < \tilde{l}_+$. The formula for J can be demonstrated via a time-dependent change of probability measure [74]. From a mathematical point of view, the lack of steepness is the hallmark of a dynamical phase transition.

Finally, we take the continuum limit. Notice that $\tilde{l}_\pm$, $l_\pm$, and $\varphi(\lambda)$ depend on ϵ. Cumbersome calculations summarized in [73] yield

$$I(w) = \lim_{\epsilon\downarrow 0}\frac{J(\epsilon w)}{\epsilon} = \sup_{\lambda\in(\lambda_-,\lambda_+)}\{w\lambda - \phi(\lambda)\} \qquad (4)$$

with $\phi(\lambda) \equiv \lim_{\epsilon\downarrow 0}\varphi(\lambda)/\epsilon$ and $\lambda_\pm \equiv \lim_{\epsilon\downarrow 0} l_\pm$. The asymptotic CGF ϕ is found to be

$$\phi(\lambda) = \frac{1+\kappa}{2} - \frac{1}{2}\sqrt{(1+\kappa)^2 - 4\mathrm{Pe}^2\lambda(1+\lambda)} \qquad (5)$$

and the primary domain is

$$\tilde{\lambda}_\pm \equiv \lim_{\epsilon\downarrow 0}\tilde{l}_\pm = -\frac{1}{2} \pm \frac{1}{2}\sqrt{1 + \left(\frac{1+\kappa}{\mathrm{Pe}}\right)^2}. \qquad (6)$$

An explicit formula for the boundary points $\lambda_\pm$ of the effective domain is not available.

According to Eq. (5), the function ϕ is not steep on the effective domain (λ_-, λ_+) when $\lambda_- > \tilde{\lambda}_-$ or $\lambda_+ < \tilde{\lambda}_+$. The lack of steepness originates linear tails of the rate function I that begin at the singular points $w_- \equiv \phi'(\lambda_-) > -\infty$ if $\lambda_- > \tilde{\lambda}_-$ and $w_+ \equiv \phi'(\lambda_-) < +\infty$ if $\lambda_+ < \tilde{\lambda}_-$. In fact, the supremum in Eq. (4) reads

$$I(w) = \begin{cases} \lambda_-(w - w_-) + i(w_-) & \text{if } w \le w_-, \\ i(w) & \text{if } w_- < w < w_+, \\ \lambda_+(w - w_+) - i(w_+) & \text{if } w \ge w_+ \end{cases}$$

with $i(w) \equiv (\sqrt{1+(w/\mathrm{Pe})^2}\sqrt{(1+\kappa)^2+\mathrm{Pe}^2} - 1 - \kappa - w)/2$. Interestingly, the smooth function i is the rate function of the entropy production at stationarity [73]. The entropy production differs from the active work by local contributions of the initial and ending points of the trajectory [73], which prevent its rate function from exhibiting singularities at stationarity [73], a circumstance that boosts the interest in the active work.

Figure 1 shows the functions ϕ and I. Figures 1(a) and 1(b) refer to the concentrated nonstationary initial condition $\sigma_r\downarrow 0$ and $\sigma_a\downarrow 0$, for which the primary and the effective domain coincide. Figures 1(c)–1(f) correspond to stationary initial conditions. At stationarity the rate function has a left

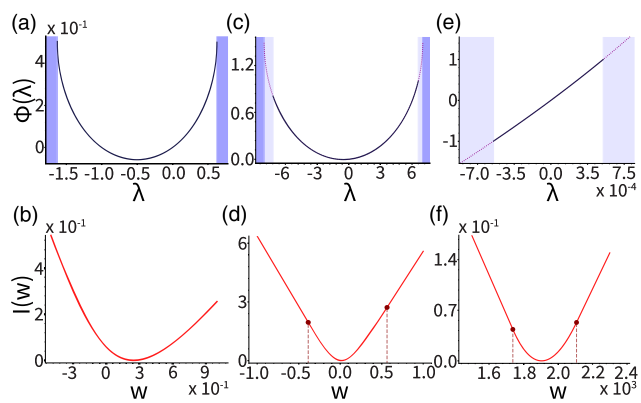

FIG. 1. Asymptotic CGF ϕ and rate function I under a concentrated nonstationary initial condition with $\sigma_r\downarrow 0$ and $\sigma_a\downarrow 0$ for $\kappa = 0.01$ and $\mathrm{Pe} = 0.5$ in (a) and (b), under the stationary initial condition with $\kappa = 2.0$ and $\mathrm{Pe} = 0.2$ in (c) and (d), and under the stationary initial condition with $\kappa = 20.0$ and $\mathrm{Pe} = 200.0$ in (e) and (f). The dark and light blue areas in (a), (c), and (e) mark the regions outside the primary and effective domain, respectively. The dotted lines in (d) and (f) mark the beginning of the left linear tail at w_- and of the right one at w_+.

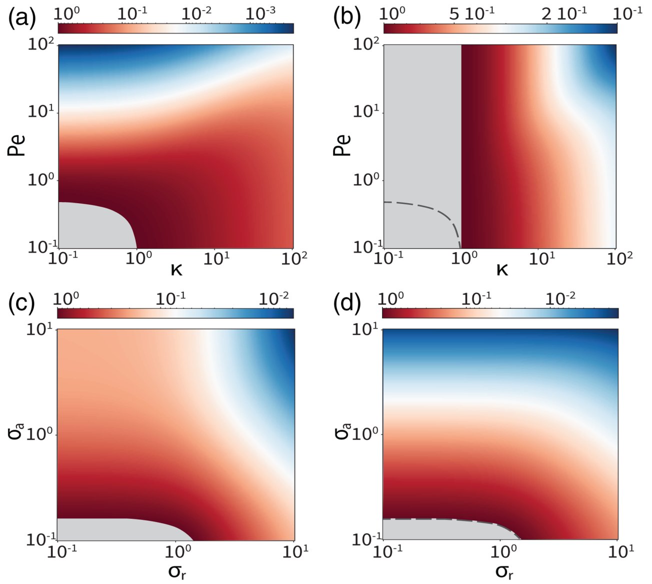

FIG. 2. Phase diagram as deduced by the ratios $r_- \equiv \lambda_-/\tilde{\lambda}_-$ and $r_+ \equiv \lambda_+/\tilde{\lambda}_+$ between the effective and primary domain boundary points of the asymptotic CGF. Colored areas denote regions where a dynamical phase transition occurs, i.e., $r_- < 1$ or $r_+ < 1$, and the color scale measures r_- and r_+. Gray areas denote regions without a singularity, i.e., $r_- = 1$ or $r_+ = 1$. (a) and (b): r_- and r_+ under the stationary initial condition in the $\kappa - \mathrm{Pe}$ plane. (c) and (d): r_- and r_+ under the nonstationary initial condition in the $\sigma_r - \sigma_a$ plane at $\kappa = 0.7$ and $\mathrm{Pe} = 0.1$ for which there is no dynamical phase transition at stationarity. The regions under the dashed lines do not exhibit any phase transition.

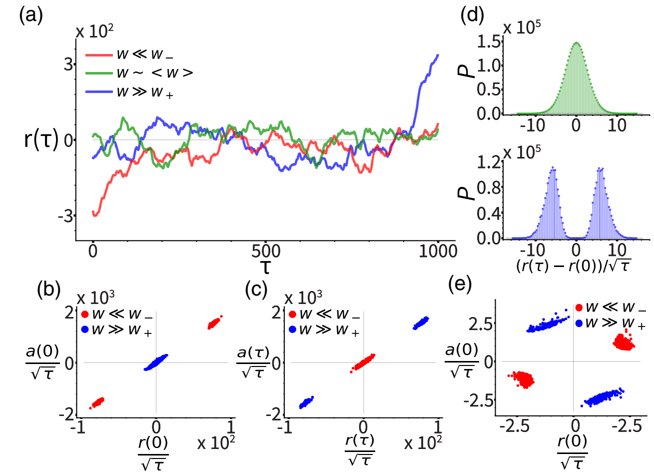

FIG. 3. Trajectory analysis at stationarity with $\kappa = 20.0$ and $\mathrm{Pe} = 200.0$ and under the nonstationary initial condition with $\kappa = 0.7$ and $\mathrm{Pe} = 0.1$. (a) Typical trajectories of the particle in the stationary configuration up to time $\tau = 10^3$ corresponding to $w = 26 \ll w_- = 1.73 \times 10^3$ (red), $w = 1.92 \times 10^3 \approx \langle w \rangle$ (green), and $w = 4.10 \times 10^3 \gg w_+ = 2.11 \times 10^3$ (blue). (b) and (c): Initial and ending points of a pool of stationary trajectories corresponding to $w \leq 8.00 \times 10^2 \ll w_-$ and $w \geq 3.20 \times 10^3 \gg w_+$, respectively. (d): stationary distribution of the net displacement conditional on typical w in the interval $-\sigma_w < w - \langle w \rangle < \sigma_w$ (top) and on large w in the interval $3\sigma_w < w - \langle w \rangle < 4\sigma_w$ (bottom), $\sigma_w \sim 2.76 \times 10^2$ being the standard deviation of the active work. (e): Initial and ending points of a pool of nonstationary trajectories with $\sigma_r = \sigma_a = 10$ and $\tau = 2 \times 10^4$ corresponding to $w \leq -5.00 \times 10^{-2} \ll w_- = 1.09 \times 10^{-3}$ and $w \geq 2.50 \times 10^{-1} \gg w_+ = 8.19 \times 10^{-2}$, respectively.

linear tail, i.e., $\lambda_- > \tilde{\lambda}_-$, for $\mathrm{Pe}\sqrt{(3+\kappa)(1+3\kappa)} > 1 - \kappa^2$ and a right linear tail, i.e., $\lambda_+ < \tilde{\lambda}_+$, for $\kappa > 1$ [73]. Figure 2 reports phase diagrams as deduced by inspecting the ratios $r_- \equiv \lambda_-/\tilde{\lambda}_-$ and $r_+ \equiv \lambda_+/\tilde{\lambda}_+$. Figures 2(a) and 2(b) show that at stationarity and at large κ and Pe the effective domain is significantly smaller than the primary domain with $\lambda_- \gg \tilde{\lambda}_-$ or $\lambda_+ \ll \tilde{\lambda}_+$, respectively. Figures 2(c) and 2(d) depict r_- and r_+ under nonstationary initial conditions for fixed values of κ and Pe such that the corresponding stationary problem has no linear tail. We find $\lambda_- \gg \tilde{\lambda}_-$ or $\lambda_+ \ll \tilde{\lambda}_+$ at large σ_r and σ_a. The results of Ref. [67] on the free AOUP are consistently recovered in the limit $\kappa \downarrow 0$ by the confined nonstationary model with $\sigma_a = \mathrm{Pe}$ [73]. Singularities of the rate function are lost in this limit.

Interpretation of the singularities of the rate function requires to analyze the particle trajectories. Figure 3(a) reports three trajectories at stationarity with large κ and Pe conditional on $W_\tau = w\tau$ with $w \ll w_-$, $w \approx \langle w \rangle$, and $w \gg w_+$. $\langle w \rangle$ is the typical value of the active work, that is $I(\langle w \rangle) = 0$. A fluctuation $w \ll w_-$ of the active work involves a short initial transient during which the particle is captured by the harmonic trap. Figure 3(b) shows that this transient is characterized by a large value of the initial position, $r(0) \sim \sqrt{\tau}$, which goes along with a large value of the initial active force, $a(0) \sim \sqrt{\tau}$, in the same direction since $r(0)$ and $a(0)$ are positively correlated by Eq. (2). Their contribution to the active work is of order $-a(0)r(0) \sim \tau$ and negative because the particle moves oppositely to the active force. In conclusion, the fluctuation $w \ll w_-$ is due to an initial transient that provides a macroscopic fraction of the active work, with the active force trying to push the particle out of the harmonic trap unsuccessfully. Specularly, a fluctuation $w \gg w_+$ entails a final short transient during which the particle escapes from the trap. In fact, Fig. 3(c) proves that there are large final values of the position and the active force, $r(\tau) \sim \sqrt{\tau}$ and $a(\tau) \sim \sqrt{\tau}$, and that they are in the same direction. Their contribution to the active work is positive and of order $a(\tau)r(\tau) \sim \tau$ since this time the active force successfully pushes the particle out of the trap. None of the above transients is observed when $w \approx \langle w \rangle$. According to Fig. 3(d), the distribution of the net displacement in a time interval τ has one peak at zero when $w \approx \langle w \rangle$ and two symmetric peaks due to final large values when $w \gg w_+$.

Finally, under the nonstationary initial condition with small κ and Pe, where dynamical phase transitions do not occur at stationarity, we observe singularities at both

$w \ll w_-$ and $w \gg w_+$. These singularities arise solely due to large values in the initial condition, $r(0) \sim \sqrt{\tau}$ and $a(0) \sim \sqrt{\tau}$ as shown by Fig. 3(e), with the particle captured by the harmonic trap providing a contribution of order $-a(0)r(0) \sim \tau$ to the active work. The latter can be either negative or positive since $r(0)$ and $a(0)$ are now uncorrelated.

The occurrence of large values of $r(0)$ and $a(0)$ or $r(\tau)$ and $a(\tau)$ is reminiscent of some big-jump phenomena observed in sums of independent random variables [21,23,28,78]. The latter works have understood that a fluctuation in the linear tail of the rate function can be decomposed in two parts: many small deviations in the same direction which sum up to the singular point, and a big jump of a single variable summing to the actual value of the fluctuation. Basically, we find that a large fluctuation of the active work is realized in a similar way through some big jumps, which localize at the initial or at the ending points of the trajectories due to the dependence structure of the process. In fact, suppose a big jump of $r(t)$ and $a(t)$ occurs at an intermediate time t, with the particle escaping the trap up to t and generating a positive active work; afterwards, the particle is bound to be recatched, and in doing so generates a negative active work that cancels out the first contribution. We mention that a crucial role of initial conditions has been recently also proven in current rate functions [79,80] and correlation functions [81,82].

In summary, we have characterized the active work large fluctuations of an AOUP in a harmonic potential. We have demonstrated that confinement can induce dynamical phase transitions at sufficiently large active and harmonic force parameters. Furthermore, we have provided an in-depth understanding of these transitions in terms of phase separation in trajectory space driven by big-jump mechanisms. These results can contribute to interpret singularities of active work rate functions in systems of interacting active Brownian particles. We plan to extend our approach to current fluctuations of several AOUPs and to problems involving AOUPs coupled via elastic forces, like active polymers [83]. Big jumps could also show up in current fluctuations, as suggested by studies on run and tumble particle systems [79].

This work has been supported by the Italian Ministry of University and Research via the project PRIN/2020 PFCXPE and by Apulia Region via the project UNIBA044 of the research programme REFIN—Research for Innovation.

[1] R. Ellis, *Entropy, Large Deviations, and Statistical Mechanics* (Springer, New York, 1985).
[2] H. Touchette, Phys. Rep. **478**, 1 (2009).
[3] A. Dembo and O. Zeitouni, *Large Deviations Techniques and Applications*, 2nd ed. (Springer, New York, 1988).
[4] F. den Hollander, *Large Deviations* (American Mathematical Society, Providence, 2000).
[5] R. L. Jack, Eur. Phys. J. B **93**, 74 (2020).
[6] T. Bodineau and B. Derrida, Phys. Rev. E **72**, 066110 (2005).
[7] R. J. Harris, A. Rákos, and G. M. Schütz, J. Stat. Mech. (2005) P08003.
[8] P. Visco, J. Stat. Mech. (2006) P06006.
[9] J. Mehl, T. Speck, and U. Seifert, Phys. Rev. E **78**, 011123 (2008).
[10] P. I. Hurtado and P. L. Garrido, Phys. Rev. Lett. **107**, 180601 (2011).
[11] L. Bertini, A. De Sole, D. Gabrielli, G. Jona-Lasinio, and C. Landim, J. Stat. Mech. (2010) L11001.
[12] M. Lefevere, R. Mariani, and L. Zambotti, J. Math. Phys. (N.Y.) **52**, 033302 (2011).
[13] G. Bunin, Y. Kafri, and D. Podolsky, Europhys. Lett. **99**, 20002 (2012).
[14] T. Speck, A. Engel, and U. Seifert, J. Stat. Mech. (2012) P12001.
[15] A. Pal and S. Sabhapandit, Phys. Rev. E **87**, 022138 (2013).
[16] T. R. Gingrich, S. Vaikuntanathan, and P. L. Geissler, Phys. Rev. E **90**, 042123 (2014).
[17] P. T. Nyawo and H. Touchette, Europhys. Lett. **116**, 50009 (2016).
[18] R. J. Harris and H. Touchette, J. Phys. A **50**, 10LT01 (2017).
[19] M. Zamparo, J. Phys. A **52**, 495004 (2019).
[20] M. Zamparo, J. Phys. A **55**, 484001 (2022).
[21] I. Jeon, P. March, and B. Pittel, Ann. Probab. **28**, 1162 (2000).
[22] S. N. Majumdar, M. R. Evans, and R. K. P. Zia, Phys. Rev. Lett. **94**, 180601 (2005).
[23] I. Armendáriz and M. Loulakis, Probab. Theory Relat. Fields **145**, 175 (2009).
[24] N. Merhav and Y. Kafri, J. Stat. Mech. (2010) P02011.
[25] J. Szavits-Nossan, M. R. Evans, and S. N. Majumdar, Phys. Rev. Lett. **112**, 020602 (2014).
[26] F. Corberi, G. Gonnella, A. Piscitelli, and M. Zannetti, J. Phys. A **46**, 042001 (2013).
[27] M. Zannetti, Europhys. Lett. **111**, 20004 (2015).
[28] C. Godréche, J. Stat. Mech. (2019) 063207.
[29] J. P. Garrahan, R. L. Jack, V. Lecomte, E. Pitard, K. van Duijvendijk, and F. van Wijland, J. Phys. A **42**, 075007 (2009).
[30] R. L. Jack and P. Sollich, Prog. Theor. Phys. Suppl. **184**, 304 (2010).
[31] J. Tailleur and J. Kurchan, Nat. Phys. **3**, 203 (2007).
[32] G. Gompper *et al.*, J. Phys. Condens. Matter **32**, 193001 (2020).
[33] J. Tailleur and M. E. Cates, Phys. Rev. Lett. **100**, 218103 (2008).
[34] P. Pietzonka, K. Kleinbeck, and U. Seifert, New J. Phys. **18**, 052001 (2016).
[35] F. Cagnetta, F. Corberi, G. Gonnella, and A. Suma, Phys. Rev. Lett. **119**, 158002 (2017).
[36] S. Whitelam, K. Klymko, and D. Mandal, J. Chem. Phys. **148**, 154902 (2018).
[37] T. GrandPre and D. T. Limmer, Phys. Rev. E **98**, 060601(R) (2018).

[38] G. Gradenigo and S. N. Majumdar, J. Stat. Mech. (2019) 053206.
[39] F. Cagnetta and E. Mallmin, Phys. Rev. E **101**, 022130 (2020).
[40] E. Fodor, T. Nemoto, and S. Vaikuntanathan, New J. Phys. **22**, 013052 (2020).
[41] D. Chaudhuri and A. Dhar, J. Stat. Mech. (2021) 013207.
[42] T. GrandPre, K. Klymko, K. K. Mandadapu, and D. T. Limmer, Phys. Rev. E **103**, 012613 (2021).
[43] N. R. Smith and O. Farago, Phys. Rev. E **106**, 054118 (2022).
[44] P. Pietzonka, E. Fodor, C. Lohrmann, M. E. Cates, and U. Seifert, Phys. Rev. X **9**, 041032 (2019).
[45] É. Fodor and M. E. Cates, Europhys. Lett. **134**, 10003 (2021).
[46] R. Di Leonardo, L. Angelani, D. Dell'Arciprete, and E. Di Fabrizio, Proc. Natl. Acad. Sci. U.S.A. **107**, 9541 (2010).
[47] G. Vizsnyiczai, G. Frangipane, C. Maggi, F. Saglimbeni, S. Bianchi, and R. Di Leonardo, Nat. Commun. **8**, 15974 (2017).
[48] S. Krishnamurthy, S. Ghosh, D. Chatterji, R. Ganapathy, and A. Sood, Nat. Phys. **12**, 1134 (2016).
[49] C. O. Reichhardt and C. Reichhardt, Annu. Rev. Condens. Matter Phys. **8**, 51 (2017).
[50] T. Nemoto, E. Fodor, M. E. Cates, R. L. Jack, and J. Tailleur, Phys. Rev. E **99**, 022605 (2019).
[51] Y.-E. Keta, E. Fodor, F. van Wijland, M. E. Cates, and R. L. Jack, Phys. Rev. E **103**, 022603 (2021).
[52] T. Agranov, M. E. Cates, and R. L. Jack, J. Stat. Mech. (2022) 123201.
[53] N. Kumar, S. Ramaswamy, and A. K. Sood, Phys. Rev. Lett. **106**, 118001 (2011).
[54] N. Kumar, H. Soni, S. Ramaswamy, and A. K. Sood, Phys. Rev. E **91**, 030102(R) (2015).
[55] G. Szamel, Phys. Rev. E **90**, 012111 (2014).
[56] C. Maggi, U. M. B. Marconi, N. Gnan, and R. Di Leonardo, Sci. Rep. **5** (2015).
[57] T. F. F. Farage, P. Krinninger, and J. M. Brader, Phys. Rev. E **91**, 042310 (2015).
[58] E. Fodor, C. Nardini, M. E. Cates, J. Tailleur, P. Visco, and F. van Wijland, Phys. Rev. Lett. **117**, 038103 (2016).
[59] L. Caprini, U. M. B. Marconi, A. Puglisi, and A. Vulpiani, J. Chem. Phys. **150**, 024902 (2019).
[60] D. Martin, J. O'Byrne, M. E. Cates, E. Fodor, C. Nardini, J. Tailleur, and F. van Wijland, Phys. Rev. E **103**, 032607 (2021).
[61] A. Crisanti and M. Paoluzzi, Phys. Rev. E **107**, 034110 (2023).
[62] M. Caraglio and T. Franosch, Phys. Rev. Lett. **129**, 158001 (2022).
[63] N. Arsha, K. P. Jepsin, and M. Sahoo, Int. J. Mod. Phys. B **37**, 2350207 (2023).
[64] G. Szamel, Phys. Rev. E **107**, 054602 (2023).
[65] S. K. Nandi and N. S. Gov, Soft Matter **13**, 7609 (2017).
[66] E. Woillez, Y. Kafri, and N. S. Gov, Phys. Rev. Lett. **124**, 118002 (2020).
[67] M. Semeraro, A. Suma, I. Petrelli, F. Cagnetta, and G. Gonnella, J. Stat. Mech. (2021) 123202.
[68] S. Das, G. Gompper, and R. G. Winkler, New J. Phys. **20**, 015001 (2018).
[69] S. Mandal, B. Liebchen, and H. Löwen, Phys. Rev. Lett. **123**, 228001 (2019).
[70] The results we present here are based on the Stratonovich prescription. We have checked that the Itô definition leads to the same findings.
[71] L. Onsager and S. Machlup, Phys. Rev. **91**, 1505 (1953).
[72] C. W. Gardiner, *Handbook of Stochastic Methods*, 3rd ed. (Springer, New York, 2003).
[73] See Supplemental Material at http://link.aps.org/supplemental/10.1103/PhysRevLett.131.158302 for additional information, which includes Refs. [67,74–76].
[74] M. Zamparo and M. Semeraro, J. Math. Phys. (N.Y.) **64**, 023302 (2023).
[75] L. Dabelow, S. Bo, and R. Eichhorn, Phys. Rev. X **9**, 021009 (2019).
[76] D.-Q. Jiang and D. Jiang, *Mathematical Theory of Nonequilibrium Steady States: On the Frontier of Probability and Dynamical Systems* (Springer Science & Business Media, New York, 2004).
[77] J. Gutierrez-Gutierrez and P. M. Crespo, IEEE Trans. Inf. Theory **54**, 5671 (2008).
[78] M. R. Evans, S. N. Majumdar, and R. K. P. Zia, J. Stat. Phys. **123**, 357 (2006).
[79] T. Banerjee, S. N. Majumdar, A. Rosso, and G. Schehr, Phys. Rev. E **101**, 052101 (2020).
[80] C. Di Bello, A. K. Hartmann, S. N. Majumdar, F. Mori, A. Rosso, and G. Schehr, Phys. Rev. E **108**, 014112 (2023).
[81] T. Banerjee, R. L. Jack, and M. E. Cates, Phys. Rev. E **106**, L062101 (2022).
[82] D. S. Dean, S. N. Majumdar, and G. Schehr, J. Stat. Mech. (2023) 063208.
[83] V. Bianco, E. Locatelli, and P. Malgaretti, Phys. Rev. Lett. **121**, 217802 (2018).